

## Coincidence Mössbauer Spectroscopic Study of $^{57}\text{Co}$ -Labelled $\text{CoSeO}_4$ and $\text{CoSeO}_4 \cdot \text{H}_2\text{O}$

Yasuo WATABABE,<sup>†</sup> Masami NAKADA, Kazutoyo ENDO,\* Hiromichi NAKAHARA, and Hirotoshi SANO  
Department of Chemistry, Faculty of Science, Tokyo Metropolitan University, Fukasawa, Setagaya, Tokyo 158  
(Received December 14, 1989)

KX-Ray-gated emission Mössbauer spectra and time-resolved emission Mössbauer spectra of  $^{57}\text{Co}$ -labelled  $\text{CoSeO}_4$  and  $\text{CoSeO}_4 \cdot \text{H}_2\text{O}$  were measured at room temperature using a coincidence technique. No difference in the area intensity ratio of  $^{57}\text{Fe(II)}$  to the sum area intensity of  $^{57}\text{Fe(II)}$  and  $^{57}\text{Fe(III)}$  was observed for anhydrous  $\text{CoSeO}_4$  between the KX-ray-gated and non-gated emission spectra; a larger area intensity of  $^{57}\text{Fe(II)}$ , however, was observed for the KX-ray-gated spectrum of  $\text{CoSeO}_4 \cdot \text{H}_2\text{O}$  than for the non-gated one. This difference is attributed to different local radiolytic effect of the deexcitation processes between KX-ray and Auger electron emission. The time-dependence in the area intensity ratio of  $^{57}\text{Fe(II)}$  to the sum area intensity of  $^{57}\text{Fe(II)}$  and  $^{57}\text{Fe(III)}$  was observed for  $\text{CoSeO}_4 \cdot \text{H}_2\text{O}$ . The relaxation process observed for  $\text{CoSeO}_4 \cdot \text{H}_2\text{O}$  by its time-resolved spectrum indicates that the radicals formed in the EC-decay oxidize  $^{57}\text{Fe(II)}$  on the time scale of the nuclear lifetime of the first excited state of  $^{57}\text{Fe}$ , and that a radical reaction plays an important role in determining the relaxation time.

Emission Mössbauer spectroscopy provides information concerning the chemical species of  $^{57}\text{Fe}$  produced from  $^{57}\text{Co}$ -labelled compounds if they have lifetimes of comparable order of magnitude to that of the Mössbauer resonance state. Spectroscopy combined with a coincidence technique provides more detailed information on the behavior of  $^{57}\text{Fe}$  atoms decayed from  $^{57}\text{Co}$  in chemical compounds. An early study of the time-resolved (delayed coincidence) Mössbauer spectroscopy suggested that this technique can be effectively applied to studying of the relaxation processes for unstable  $^{57}\text{Fe}$  species formed through EC-decay in insulating materials.<sup>1–4)</sup> Since the pioneering work, little progress has been made for chemical compounds. Grimm et al. showed the lifetimes of unstable high-spin  $\text{Fe(II)}$ -species formed in  $^{57}\text{Co}$ -labelled  $[\text{Co(phen)}_3](\text{ClO}_3)_2 \cdot 2\text{H}_2\text{O}$  at various temperatures.<sup>5)</sup>

A KX-ray-gated emission Mössbauer spectrum (X,  $\gamma$ -ray coincidence spectrum) gives information concerning the various chemical effects associated with KX-ray emission during the deexcitation process in EC-decay. Kobayashi and co-workers found different distributions of  $\text{Fe(II)}$  and  $\text{Fe(III)}$  between KX-ray-gated and non-gated emission Mössbauer spectra of  $^{57}\text{Co}$ -labelled  $\text{CoCl}_2 \cdot n\text{H}_2\text{O}$  ( $n=2, 4$ , and  $6$ ); they interpreted it as being based on the different local radiolytic effects during deexcitation (i.e., different chemical effects of KX-ray and Auger electron emission).<sup>6–9)</sup>

In the present work, the KX-ray-gated emission Mössbauer spectra and the time-resolved spectra of  $^{57}\text{Co}$ -labelled  $\text{CoSeO}_4$  and  $\text{CoSeO}_4 \cdot \text{H}_2\text{O}$  were measured at room temperature using a coincidence technique. Both selenate and the hydrate were selected for the following reason. Ladorière et al. reported regarding their Mössbauer spectroscopic study that the  $\text{Fe(II)}$  salt is sensitive to  $^{60}\text{Co}$   $\gamma$ -ray irradiation, and

that the conventional emission Mössbauer spectrum of  $^{57}\text{Co}$ -labelled cobalt(II) salt is sensitive to water of crystallization.<sup>10)</sup> Such salts are suitable for examining in detail the various chemical effects associated with deexcitation in both EC-decay and relaxation of the nucleogenic  $^{57}\text{Fe}$ -species formed in solids.

### Experimental

**Preparation of  $^{57}\text{Co}$ -Labelled  $\text{CoSeO}_4$  and  $\text{CoSeO}_4 \cdot \text{H}_2\text{O}$ :** Cobalt(II) selenate and the hydrate were prepared by a procedure described in the literature<sup>11)</sup> with a modification for small-scale synthesis. Cobalt(II) carbonate containing  $^{57}\text{Co}$  was prepared from aqueous solutions of cobalt(II) chloride and sodium carbonate. To the aqueous suspension of freshly prepared  $^{57}\text{Co}$ -labelled  $\text{CoCO}_3 \cdot 6\text{H}_2\text{O}$ , a stoichiometric amount of selenic acid was poured under stirring. Ethanol was added to precipitate the cobalt(II) selenate. A thermogravimetric analysis and a powdered X-ray diffraction analysis proved that the salt prepared by the same procedure, but without  $^{57}\text{Co}$ , was  $\text{CoSeO}_4 \cdot 5\text{H}_2\text{O}$ .  $^{57}\text{Co}$ -labelled  $\text{CoSeO}_4 \cdot \text{H}_2\text{O}$  was obtained by heating pentahydrate at  $130^\circ\text{C}$  for 15 min under a nitrogen atmosphere. Anhydrous  $^{57}\text{Co}$ -labelled  $\text{CoSeO}_4$  was obtained upon heating monohydrate at  $300^\circ\text{C}$  for 15 min. The radioactivity was estimated to be about 200 kBq for each compound. Iron(II) selenate monohydrate and the pentahydrate were prepared by a method described in the literature.<sup>11)</sup>

**Gamma-Ray Irradiation:**  $\text{FeSeO}_4 \cdot \text{H}_2\text{O}$ ,  $\text{FeSeO}_4 \cdot 5\text{H}_2\text{O}$ ,  $\text{CoSeO}_4$ ,  $\text{CoSeO}_4 \cdot \text{H}_2\text{O}$  were irradiated with gamma-rays in air at room temperature under a dose rate of  $1.0 \times 10^6 \text{ R h}^{-1}$  with a  $^{60}\text{Co}$  source of  $3.7 \times 10^6 \text{ GBq}$  at the Inter-University Laboratory for Common Use of Japan Atomic Energy Research Institute (Tokai). The irradiated samples were stored at  $-20^\circ\text{C}$  until Mössbauer and IR measurements could be carried out.

**Measurement (1) Conventional Mössbauer Spectra:** The absorption Mössbauer spectra of iron(II) selenate were measured at room temperature against a  $^{57}\text{Co(Rh)}$  source. The conventional emission Mössbauer spectra (non-gated spectra) were observed at room temperature against an  $^{57}\text{Fe}$ -enriched stainless-steel (SUS310) foil moving in a constant

<sup>†</sup> Present address: Energy Sector, The Fuji Electric Company, Hino-city, Tokyo 191.

acceleration mode. A Wissel Mössbauer spectrometer; an MA260 transducer, a DFG1200 digital function generator and a MDU1200 Mössbauer driving unit were used for measuring all of the absorption and emission Mössbauer spectra.

**(2) X, $\gamma$ -Ray Coincidence Mössbauer Spectra:** The X, $\gamma$ -ray coincidence system used in the present experiment was essentially the same as that reported previously.<sup>12-14</sup> A NaI(Tl) crystal (0.7 mm in thick and 1 inch (1 inch=2.45 cm) in diameter) was used to detect 6.3 keV KX-rays and a NaI(Tl) crystal (1 mm in 1 thick and 1 inch in diameter) was used for 14.4 keV  $\gamma$ -rays. They were coupled to a hybrid-type photomultiplier (HAMAMATSU-H1949) and to a photomultiplier (HAMAMATSU-R329), respectively. The range of the time-to-pulse height converter (ORTEC-467) was set to 0.4  $\mu$ s. The time window was sufficiently wide to eliminate any time-filtering effect. The fraction of random coincidences was estimated to be 30–35% from the time distribution of the KX-ray and 14.4 keV  $\gamma$ -ray.

**(3) Time-Resolved Mössbauer Spectra:** The time-resolved Mössbauer spectra were observed using a delayed-coincidence technique. A block diagram of the measuring system is shown in Fig. 1. A NaI(Tl) crystal (1 inch thick and 1 inch in diameter) was used to detect 122 keV  $\gamma$ -rays, and another crystal (0.8 mm thick and 1 inch in diameter) for 14.4 keV  $\gamma$ -rays. Anode signals of the latter photomul-

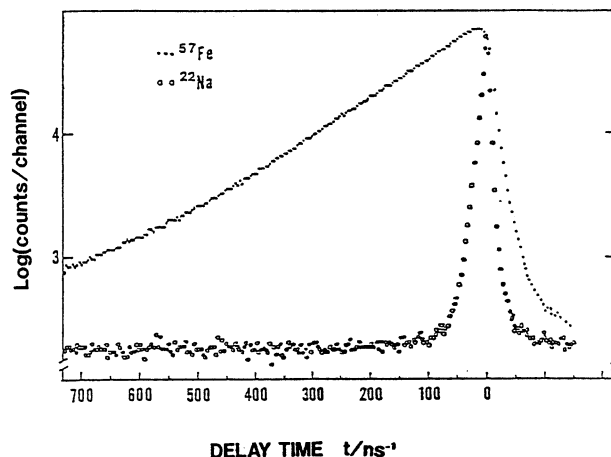


Fig. 2. Time distribution of the first excited state of  $^{57}\text{Fe}$ . Time distribution of the system was measured with the Compton scattered radiation of  $^{22}\text{Na}$  under the same conditions as the Mössbauer measurement.

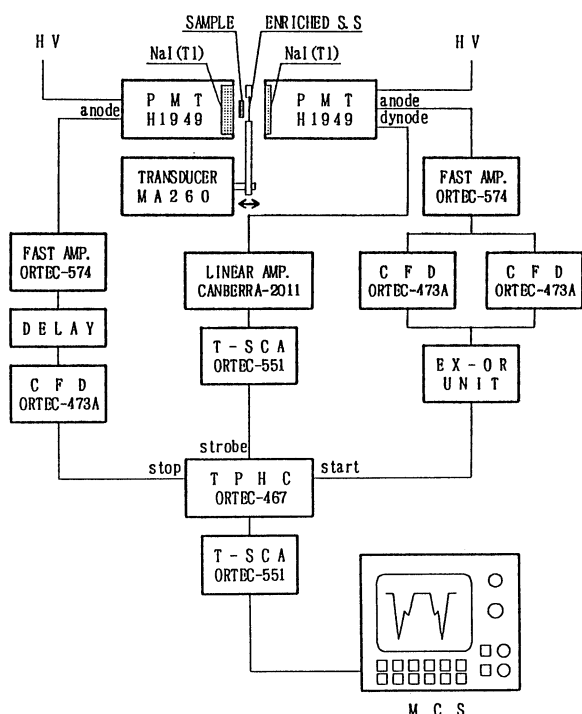


Fig. 1. Block diagram of the equipment for measuring the time-resolved Mössbauer spectra.  $^{57}\text{Fe}$ -enriched stainless steel (SUS310) was used as an absorber. The Mössbauer spectrometer was composed of the Wissel Mössbauer system (MA260 transducer, DFG1200 digital function generator, and MDU1200 driving unit) and the ORTEC-NORLAND 5500 multichannel analyzer. The ORTEC NIM modules were used for the coincidence system. An Ex-OR circuit was built by us using ECL-gates.

tiplier were fed into a fast amplifier (ORTEC-574); the outputs were then fed into two constant-fraction discriminators (ORTEC-473A). The discrimination levels were set to select signals just above 14.4 keV and just below the energy, respectively. The outputs from the discriminators were fed into an Exclusive-OR circuit developed by us using ultrafast ECL-gates. These two ORTEC-473A's and the Exclusive-OR circuit constitutes a fast single-channel discriminator. The time distribution of the first excited state of  $^{57}\text{Fe}$  is shown in Fig. 2, where the randomly coincided fraction was already subtracted. The contribution of the random coincidence on the time distribution was nearly 10% at the peak position, and 50% (a true-to-random coincidence ratio 1:1) at a delay time of 250 ns. The time resolution (FWHM) of the equipment was  $10.5 \pm 0.4$  ns when it was measured with the Compton scattered radiation of  $^{22}\text{Na}$ . The time-resolved Mössbauer spectrum was obtained by subtracting randomly coincided fractions from the observed coincided Mössbauer spectrum.

**Analysis:** The conventional and time-resolved spectra of  $^{57}\text{Co}$ -labelled  $\text{CoSeO}_4$  were analyzed with three sets of quadrupole doublets: two sets were for Fe(II) and the other set for Fe(III); those of  $^{57}\text{Co}$ -labelled  $\text{CoSeO}_4 \cdot \text{H}_2\text{O}$  were analyzed with two sets of quadrupole doublets using a least-square fitting program. Lorentzian functions were used for the conventional emission and absorption spectra, while Gaussian functions were used for the time-resolved spectra, based on the favorable  $\chi^2$  values. The time-filtering effects were ignored in an analysis of the time-resolved Mössbauer spectra,<sup>15,16</sup> since the time-windows selected were rather wide; also, the oscillations in the actual emission spectra were averaged due to the various kinds of relaxation caused by aftereffects in such insulator-type chemical compounds.

## Results

**Conventional Emission Mössbauer Spectra.** The conventional emission spectra of  $^{57}\text{Co}$ -labelled  $\text{CoSeO}_4 \cdot \text{H}_2\text{O}$  and  $\text{CoSeO}_4 \cdot 5\text{H}_2\text{O}$  were measured at room temperature; the parameters are listed in Table 1. The spec-

Table 1. Parameters for Non-Gated and KX-Ray-Gated Emission Mössbauer Spectra of  $^{57}\text{Co}$ -Labelled  $\text{CoSeO}_4$ ,  $\text{CoSeO}_4 \cdot \text{H}_2\text{O}$ , and  $\text{CoSeO}_4 \cdot 5\text{H}_2\text{O}$  at Room Temperature

	Non-Gated			Rel.int. <sup>a)</sup> %	Rel.area. <sup>b)</sup> %	Gated			Rel.int. <sup>a)</sup> %	Rel.area. <sup>b)</sup> %
	IS	QS	FWHM			IS	QS	FWHM		
	mm s <sup>-1</sup>	mm s <sup>-1</sup>	mm s <sup>-1</sup>			mm s <sup>-1</sup>	mm s <sup>-1</sup>	mm s <sup>-1</sup>		
<b>CoSeO<sub>4</sub></b>										
Fe(II)-1	1.38(1) <sup>c)</sup>	3.36(2)	0.98(2)	3.56(10)	27.6(14)	1.38(3)	3.38(4)	0.99(4)	3.90(23)	24.0(27)
Fe(II)-2	1.11(1)	3.06(2)	0.84(2)	2.64(8)	17.9(19)	1.10(2)	3.06(5)	0.91(3)	3.39(25)	19.2(25)
Fe(III)	0.37(1)	1.29(2)	0.89(3)	7.03(22)	54.5(20)	0.36(3)	1.26(4)	1.11(4)	6.29(32)	56.8(29)
<b>CoSeO<sub>4</sub> · H<sub>2</sub>O</b>										
Fe(II)	1.24(1)	2.71(2)	0.73(1)	2.47(4)	19.1(9)	1.26(3)	2.70(6)	0.86(4)	2.85(40)	24.1(22)
Fe(III)	0.30(1)	1.11(2)	0.83(1)	9.24(10)	80.9(17)	0.33(3)	0.95(5)	1.21(3)	9.40(40)	75.9(28)
<b>CoSeO<sub>4</sub> · 5H<sub>2</sub>O</b>										
Fe(II)	1.22(2)	3.10(2)	0.89(3)	1.52(6)	9.3(10)					
Fe(III)	0.23(3)	0.88(5)	1.20(5)	11.22(11)	90.7(20)					

a) Relative intensity of absorption. b) Relative area. c) Values in parenthesis indicate errors on lowest one or two figures.

trum shows nearly a 90% yield of  $^{57}\text{Fe(III)}$  species for  $\text{CoSeO}_4 \cdot 5\text{H}_2\text{O}$ , while 80.9% of the  $^{57}\text{Fe(III)}$  species for  $\text{CoSeO}_4 \cdot \text{H}_2\text{O}$  and 54.5% for anhydrous  $\text{CoSeO}_4$ . It is reported that  $\text{CoSeO}_4 \cdot 5\text{H}_2\text{O}$  shows the same crystal structure as  $\text{CuSO}_4 \cdot 5\text{H}_2\text{O}$ . Four water molecules coordinate to the cobalt(II) ion, and one water molecule links through a hydrogen bond to the two selenate ions. The water molecules coordinated to  $^{57}\text{Co(II)}$  decompose through EC-decay, resulting in the formation of OH radicals. These oxidize the nucleogenic  $^{57}\text{Fe(II)}$ . In a chemical synthesis,  $\text{FeSeO}_4 \cdot 5\text{H}_2\text{O}$  is formed from an aqueous solution and the monohydrate is obtained by heating the pentahydrate at 105 °C under a nitrogen atmosphere. Further heating of monohydrate at 110 °C results in the decomposition of selenate ions without forming anhydrous  $\text{FeSeO}_4$ . It is, therefore, hardly possible to prepare  $\text{FeSeO}_4$  through normal chemical synthesis. Even if it is impossible to do by chemical synthesis, the emission Mössbauer spectrum of  $^{57}\text{Co}$  enables us to show the chemical states of  $^{57}\text{Fe}$ -species decayed from a  $^{57}\text{Co}$ -labelled compound on the time scale ( $10^{-7}$  s) as the first excited state of  $^{57}\text{Fe}$  nucleus.

**KX-Ray-Gated Mössbauer Spectra.** The KX-ray-gated Mössbauer spectra of  $^{57}\text{Co}$ -labelled  $\text{CoSeO}_4$  and  $\text{CoSeO}_4 \cdot \text{H}_2\text{O}$  are shown in Fig. 3 together with the conventional emission spectra at room temperature for a comparison. No difference in the area intensity ratio of  $^{57}\text{Fe(II)}$  to the sum area of  $^{57}\text{Fe(II)}$  and  $^{57}\text{Fe(III)}$  was observed for anhydrous  $\text{CoSeO}_4$  between the KX-ray-gated and non-gated emission spectra, while a larger relative intensity of  $^{57}\text{Fe(II)}$  was observed for the KX-ray-gated spectrum of  $\text{CoSeO}_4 \cdot \text{H}_2\text{O}$  than for non-gated one. In the KX-ray emission, multiple ionization is less pronounced than Auger electron emission. The redistribution of electronic states after KX-ray emission does not cause a very large perturbation in the electronic shells of  $^{57}\text{Fe}$  and the neighbouring atoms as does the competitive Auger process in the vicinity of the decayed  $^{57}\text{Fe}$  atoms. This leads to the

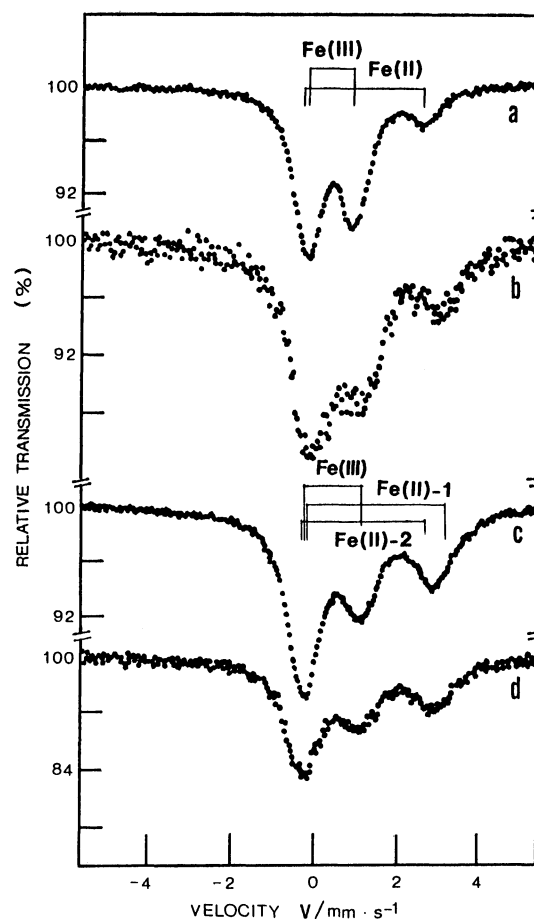


Fig. 3. Conventional emission Mössbauer spectra of  $^{57}\text{Co}$ -labelled (a)  $\text{CoSeO}_4 \cdot \text{H}_2\text{O}$  and (c)  $\text{CoSeO}_4$ , and the KX-ray-gated emission spectra of (b)  $\text{CoSeO}_4 \cdot \text{H}_2\text{O}$  and  $\text{CoSeO}_4$  at room temperature.

formation of oxidizing radicals in smaller amounts during KX-ray emission and the subsequent deexcitation processes. This must be the reason for the larger fraction of  $^{57}\text{Fe(II)}$ -species during the KX-ray emission process than during Auger electron emission. In the case of anhydrous  $\text{CoSeO}_4$ , however, the

chemical distribution of  $^{57}\text{Fe(II)}$  was found to be the same for both non-gated and gated spectra. These results indicate the same trends regarding  $\text{CoF}_2$  and  $\text{CoF}_2 \cdot 2\text{H}_2\text{O}$ .<sup>17)</sup> The Auger electron emission process in the labelled compound with the water of crystallization produces the  $^{57}\text{Fe(III)}$ -species in large amount. These results strongly indicate that the oxidizing radicals are formed as radiolytic process of the water molecule in EC-decay. In a previous study, we confirmed that radical formation occurs in the vicinity of decayed  $^{57}\text{Fe}$  in many labelled compounds.<sup>18–23)</sup> Local radiolysis takes place in both the selenate anion and in the water of crystallization through EC-decay. It is, however, noted that the OH radicals formed during the radiolytic process of the water molecule is much more effective for oxidizing the decayed  $^{57}\text{Fe(II)}$ -species than selenate ions in the present experiment.

**Time-Resolved Spectra of  $^{57}\text{Co}$ -Labelled Anhydrous  $\text{CoSeO}_4$ .** The time-resolved emission Mössbauer spectra of  $^{57}\text{Co}$ -labelled  $\text{CoSeO}_4$  are shown in Fig. 4. The area ratio of  $^{57}\text{Fe(II)-1}$ ,  $^{57}\text{Fe(II)-2}$  and the sum area ratio of  $^{57}\text{Fe(II)-1}$  and  $^{57}\text{Fe(II)-2}$  to the total area of the spectrum are depicted in Fig. 5. The relative area of the  $^{57}\text{Fe(II)-1}$  species with a large QS value did not change upon the delay time, while that of the  $^{57}\text{Fe(II)-2}$  species with a small QS value increased. It has been

reported in an ESR study of gamma-ray irradiated  $\text{K}_2\text{SeO}_4$  that gamma-ray induced radiolysis gave rise to such radicals as  $\text{SeO}_4^{2-}$ ,  $\text{SeO}_3^{2-}$ , and  $\text{SeO}_2^{2-}$  and that the selenite radicals have a lifetime of 4.5 h at room temperature.<sup>24,25)</sup> In fact, the IR spectra indicated that selenite ions (a characteristic stretching vibration;  $720\text{ cm}^{-1}$ ) are formed by the irradiation of  $^{60}\text{Co}$  gamma-rays for  $\text{CoSeO}_4$ ,  $\text{CoSeO}_4 \cdot \text{H}_2\text{O}$  and  $\text{CoSeO}_4 \cdot 5\text{H}_2\text{O}$  at room temperature and that a relatively stronger intensity of the absorption peak was observed for selenate with a greater number of water molecules. This may suggest that the strongly oxidizing OH radicals formed by  $\gamma$ -ray irradiation help in the formation of selenite ions. The time-resolved emission Mössbauer spectra of anhydrous  $\text{CoSeO}_4$  showed an increase in the relative area intensity of  $^{57}\text{Fe(II)-2}$  with the delay time. The chemical states of  $^{57}\text{Fe}$ -atoms responsible for Fe(II)-1 and Fe(II)-2 are not known at present, since the corresponding Fe(II) salt has not been synthesized. However, the present results may suggest that the decayed  $^{57}\text{Fe(II)-2}$  species may be stable in a solid, at least within the Mössbauer time scale, if the environmental lattice of the decayed  $^{57}\text{Fe}$ -atoms remains as the same type structure as the  $\text{CoSeO}_4$  matrix. In the case of  $\text{CoSeO}_4$  the radicals formed through EC-decay in the vicinity are not sufficiently strong to oxidize the  $^{57}\text{Fe(II)}$ ; therefore, two-valence states formed through EC-decay exist.

**Time-Resolved Spectra of  $^{57}\text{Co}$ -Labelled  $\text{CoSeO}_4 \cdot \text{H}_2\text{O}$ .** The time-resolved emission Mössbauer spectra of  $^{57}\text{Co}$ -labelled  $\text{CoSeO}_4 \cdot \text{H}_2\text{O}$  are shown in Fig. 6 and the results are listed in Table 2. The time dependence on the ratio of the area of the  $^{57}\text{Fe(II)}$  to the sum area of  $^{57}\text{Fe(II)}$  and  $^{57}\text{Fe(III)}$  was observed for  $\text{CoSeO}_4 \cdot$

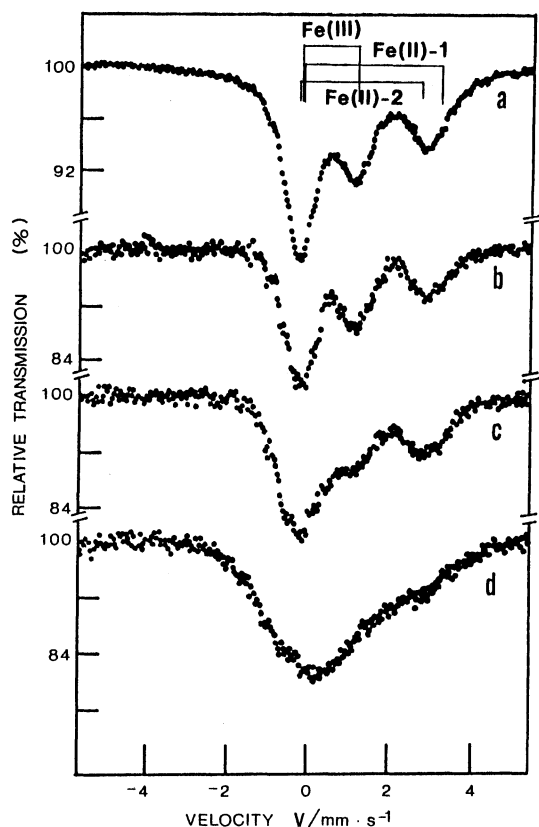


Fig. 4. Time-resolved Mössbauer spectra of  $^{57}\text{Co}$ -labelled  $\text{CoSeO}_4$  at room temperature. The time windows of the spectra are (a) random coincidence, (b) 75–140 ns, (c) 20–75 ns, (d) 0–20 ns, respectively.

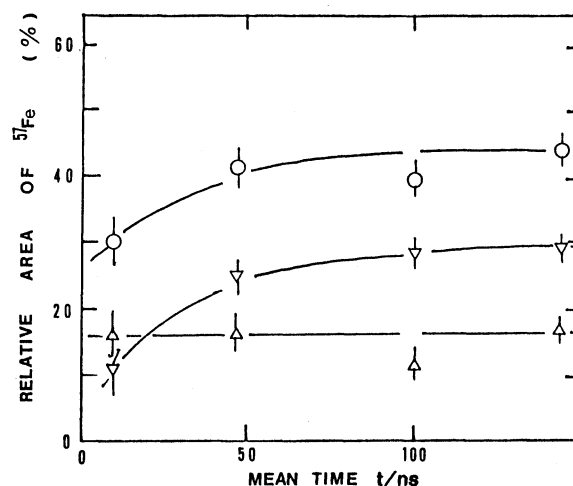


Fig. 5. The area ratios of  $^{57}\text{Fe(II)-1}$ ,  $^{57}\text{Fe(II)-2}$ , and the sum area of  $^{57}\text{Fe(II)-1}$ ,  $^{57}\text{Fe(II)-2}$ , to the total absorption area observed for  $^{57}\text{Co}$ -labelled  $\text{CoSeO}_4$  at room temperature plotted against the mean time of the preset time window: O, the ratio of the sum area of  $^{57}\text{Fe(II)-1}$  and  $^{57}\text{Fe(II)-2}$  to the total area;  $\Delta$ , the relative area of  $^{57}\text{Fe(II)-1}$ ;  $\nabla$ , the relative area of  $^{57}\text{Fe(II)-2}$ .

Table 2. Parameters for Time-Resolved Spectra of  $^{57}\text{Co}$ -Labelled  $\text{CoSeO}_4 \cdot \text{H}_2\text{O}$  at Room Temperature

Time window (Mean time/ns)	$^{57}\text{Fe(II)}$		$^{57}\text{Fe(III)}$	
	FWHM/mm s $^{-1}$	Rel.area/% <sup>a)</sup>	FWHM/mm s $^{-1}$	Rel.area/% <sup>a)</sup>
0—20 (10)	3.80 (6) <sup>b)</sup>	49.4 (39)	2.31 (4)	50.6 (40)
35—60 (47)	2.72 (3)	35.4 (30)	2.21 (2)	64.6 (25)
77—123 (100)	0.90 (2)	19.6 (18)	1.05 (2)	80.4 (32)
125—180 (151)	0.72 (2)	20.4 (21)	0.76 (2)	79.6 (32)
180—302 (223)	0.48 (1)	18.8 (21)	0.61 (2)	81.2 (23)
Conventional (144)	0.73 (1)	19.1 (9)	0.83 (1)	80.9 (17)

a) Relative area. b) Values in parenthesis indicate errors on lowest one or two figures.

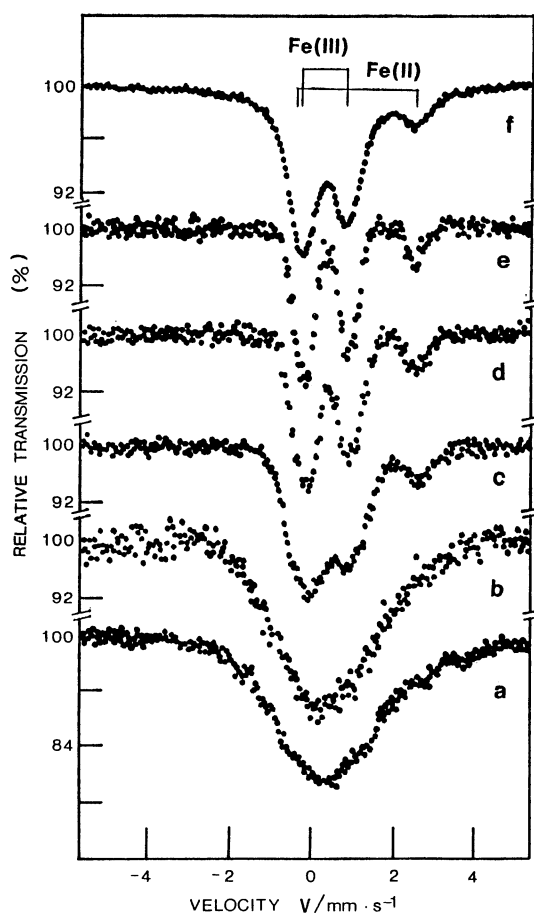


Fig. 6. Time-resolved Mössbauer spectra of  $^{57}\text{Co}$ -labelled  $\text{CoSeO}_4 \cdot \text{H}_2\text{O}$  at room temperature; (a) 0—20 ns, (b) 35—60 ns, (c) 77—123 ns, (d) 125—180 ns, (e) 180—302 ns, (f) (random coin.).

$\text{H}_2\text{O}$ , as shown in Fig. 7. The relaxation of  $^{57}\text{Fe(II)}$  observed for  $\text{CoSeO}_4 \cdot \text{H}_2\text{O}$  is analyzed in the following way. The mean time,  $t$ , for the time window between  $T_A$  and  $T_B$  was evaluated using the equation

$$t/\tau_N = \int_{T_A}^{T_B} T e^{-T} dT / \int_{T_A}^{T_B} e^{-T} dT,$$

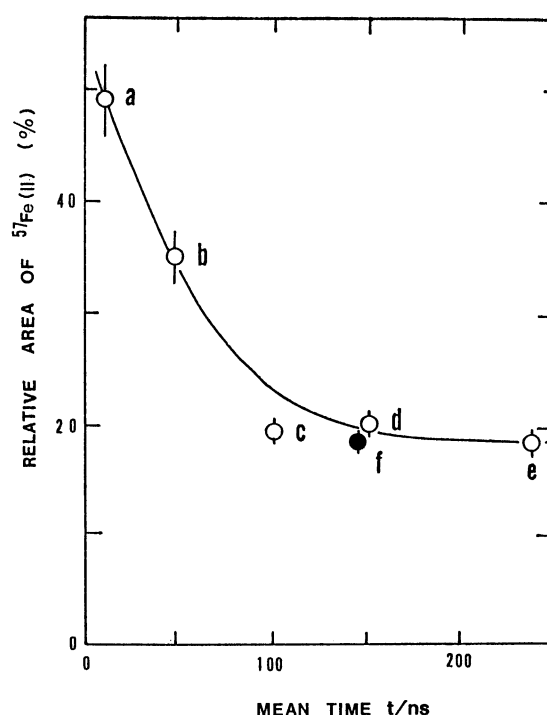
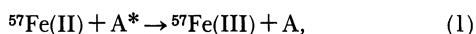


Fig. 7. Distribution of  $^{57}\text{Fe(II)}/[^{57}\text{Fe(II)}+^{57}\text{Fe(III)}]$  of  $^{57}\text{Co}$ -labelled  $\text{CoSeO}_4 \cdot \text{H}_2\text{O}$  against the mean time of the preset time window; (a) 0—20 ns, (b) 35—60 ns, (c) 77—123 ns, (d) 125—180 ns, (e) 180—302 ns, (f) (random coincidence).

where  $\tau_N$  is the mean lifetime of  $^{57}\text{Fe}$  nucleus;  $T$ ,  $T_A$  and  $T_B$  are expressed in  $\tau_N$  units. Some assumptions have to be made in order to simplify the analysis, as previously reported,<sup>14)</sup> and were somewhat changed in the present work. Debye-Waller factors of the  $^{57}\text{Fe(II)}$ - to  $^{57}\text{Fe(III)}$ -species were assumed to be the same in each time window; the ratio of the area of  $^{57}\text{Fe(II)}$  to the sum area of the  $^{57}\text{Fe(II)}$  and  $^{57}\text{Fe(III)}$  was assumed to be the same as the distribution ratio of  $^{57}\text{Fe}$ -atoms. The following reaction scheme is assumed to be the rate-determining step:



where  $\text{A}^*$  represents oxidizable radicals formed in the vicinity of the decayed  $^{57}\text{Fe}$  through EC-decay. If  $\text{A}^*$  is of sufficient amounts, at least in the time scale of  $^{57}\text{Fe}(\text{II})$  or the  $^{57}\text{Fe}$  nuclear lifetime, reaction (1) can be treated as the pseudo-first-order kinetics of a chemical decay constant,  $\lambda_c$  and the  $^{57}\text{Fe}(\text{III})$ -species, once formed, are assumed to be stable. Let the quantities of  $^{57}\text{Fe}(\text{II})$  and  $^{57}\text{Fe}(\text{III})$  at  $t$  after the emission of 122 keV gamma-rays be  $P_2(t)$  and  $P_3(t)$ , respectively. Then, the quantities of  $^{57}\text{Fe}(\text{II})$  and  $^{57}\text{Fe}(\text{III})$  at time  $t$  can be described as

$$P_2(t) + P_3(t) = 1, \quad (2)$$

and

$$P_2(t) = [P_2(0) - P_2(\infty)] \exp(-\lambda_c t) + P_2(\infty). \quad (3)$$

The fraction of  $^{57}\text{Fe}(\text{III})$ ,  $P_3(t)$ , is assumed to increase during measurements. Since emission Mössbauer spectroscopy gives information regarding the chemical states of nucleogenic atoms, the observable spectrum indicates the chemical quantities multiplied by  $\exp(-\lambda_N t)$ , where  $\lambda_N$  is the nuclear decay constant. The intensity of a time-resolved Mössbauer spectrum indicates the partially integrated quantities of Eqs. 2 or 3 with respect to the preset time window. Then, the actual intensity,  $I_i$ , ( $i=2$  and  $3$ ) of  $P_2(t)$  and  $P_3(t)$  at the time window between  $T_A$  and  $T_B$  can be described as

$$I_i = \int_{T_A}^{T_B} \left[ \int_0^\infty \lambda_N P_i(t) e^{-\lambda_N t} G(2\tau_0; t - t') dt' \right] dt. \quad (4)$$

A Gaussian function,

$$G(2\tau_0, t - t') = \frac{1}{\sqrt{2\pi(2\tau_0)^2}} \exp \left\{ -\frac{(t - t')^2}{(2\tau_0)^2} \right\},$$

was assumed for the time resolution of the equipment. As a numerical value,  $10.5 \pm 0.4$  ns was used for the present analysis. Then, the ratio of the  $^{57}\text{Fe}(\text{II})$  area to the sum area of  $^{57}\text{Fe}(\text{II})$  and  $^{57}\text{Fe}(\text{III})$  is shown as  $I_2/(I_2 + I_3)$  at a given time window. A numerical computer calculation of  $I_2/(I_2 + I_3)$  yielded the best value for  $P_2(0)$  to be  $(56.5 \pm 2.5)\%$  and the chemical decay constant,  $\lambda_c = (1.94 \pm 0.12) \times 10^{-2} \text{ ns}^{-1}$  (or the mean lifetime to be  $51.6 \pm 3.3$  ns) for the rapidly decaying  $^{57}\text{Fe}(\text{II})$  species;  $P_2(\infty)$  was shown to be  $(19.1 \pm 1.9)\%$ . The rapidly decaying fraction is ascribed to oxidation by radicals (mainly OH radicals as shown in Eq. 1);  $P_2(\infty)$  is the fraction that does not suffer from local radiolytic oxidation for the monohydrate.

### Discussion

Electron capture is accompanied by the ejection of an electron from the K- (or L-, M-,....) shell giving rise to the formation of an excited atom. This excitation can be removed either via radiative transitions in which the vacancy transfers from the K- to L-shell, then to the M-shell, or through radiationless transitions (Auger processes) involving transfer of the

vacancy to a higher shell, together with a simultaneous emission of electrons. Radiationless transitions produce a cascade of more vacancies in the electron shells than does the radiative transition.

Although multiply charged states as a result of EC-decay have been observed for  $^{37}\text{Ar}$  or  $^{133}\text{Xe}$  in the gaseous phase the lifetime depends strongly on the gaseous pressure.<sup>26)</sup> However, in a solid neutralization of a highly-charged atom occurs within such a short time (ca.  $10^{-12}$  s) that it is hardly possible to follow the process using the present measurements. Triftshäuser and Craig<sup>1)</sup> measured the time-resolved spectra of  $^{57}\text{Co}$ -labelled  $\text{CoCl}_2 \cdot 4\text{H}_2\text{O}$ ,  $\text{CoO}$ ,  $\text{CoSO}_4 \cdot 7\text{H}_2\text{O}$ ,  $(\text{NH}_4)_2\text{Fe}(\text{SO}_4)_2 \cdot 6\text{H}_2\text{O}$  and concluded that the intensity ratio of  $\text{Fe}^{2+}/\text{Fe}^{3+}$  did not change for the preset time window (i.e., 4—43, 43—86, 86—146, and 146—200 ns). They inferred that the lifetimes of the metastable states are much longer than the lifetime of a  $^{57}\text{Fe}$  nucleus, if they are formed during EC-decay.

In the present experiment, in the case of anhydrous  $^{57}\text{Co}$ -labelled  $\text{CoSeO}_4$ , many kinds of radicals or meta-stable species may have been formed in an analogous way as in the case of gamma-ray irradiated  $\text{K}_2\text{SeO}_4$ . The  $^{57}\text{Fe}$ -species formed through EC-decay may have different hyperfine parameters, and probably have long lifetimes in the absence of water of crystallization. It must be added that some short transient species decay (including electronically excited states) into other species within the Mössbauer lifetime. This would be one of the possible reasons for the apparently complicated dependence of the total  $\text{Fe}(\text{II})$  area to the total  $\text{Fe}(\text{II})$  and  $\text{Fe}(\text{III})$  upon the delay time. However, as mentioned previously, the IR data concerning gamma-ray irradiated  $\text{K}_2\text{SeO}_4$ ,  $\text{FeSeO}_4 \cdot 5\text{H}_2\text{O}$ ,  $\text{CoSeO}_4$ , and  $\text{CoSeO}_4 \cdot \text{H}_2\text{O}$  indicated the formation of selenite ions. The Mössbauer parameters suggest that  $\text{Fe}(\text{III})$ -species are formed in  $\text{FeSeO}_4 \cdot n\text{H}_2\text{O}$  ( $n=1$  or  $5$ ) by gamma-ray irradiation. If local radiolysis of EC-decay is similar to the chemical effects of  $\gamma$ -ray irradiation, the transient species of  $^{57}\text{Fe}$ -atoms formed in  $^{57}\text{Co}$ -labelled anhydrous  $\text{CoSeO}_4$  would be stabilized either to  $^{57}\text{Fe}(\text{III})$  or  $^{57}\text{Fe}(\text{II})$ . In the case of monohydrate, one fraction of the  $^{57}\text{Fe}(\text{II})$  formed through EC-decay is oxidized by OH radicals, which is responsible for the rapid decrease in the intensity of  $^{57}\text{Fe}(\text{II})$  (see Fig. 7); another remains unchanged within the present experiment. This may be the fraction that escaped from a reaction with OH radicals.

### Conclusion

The role of the water of crystallization for determining the chemical distribution of the  $^{57}\text{Fe}(\text{II})$  species formed through EC-decay in labelled  $\text{CoSeO}_4$  and  $\text{CoSeO}_4 \cdot \text{H}_2\text{O}$  was demonstrated using a coincidence technique. No difference in the area intensity ratio of  $^{57}\text{Fe}(\text{II})$  to the sum area intensity of  $^{57}\text{Fe}(\text{II})$  and  $^{57}\text{Fe}(\text{III})$  was observed for anhydrous  $\text{CoSeO}_4$  between

the X-ray-gated and the non-gated spectra. A relatively large intensity of  $^{57}\text{Fe(II)}$  was found for the KX-ray-gated emission spectrum of  $\text{CoSeO}_4 \cdot \text{H}_2\text{O}$  compared to the non-gated one. This difference is explained in terms of different local radiolytic effects of the deexcitation processes between X-ray and Auger electron emission. It is inferred in the present work that EC-decay and the following deexcitation processes give rise to such radicals as OH and  $\text{SeO}_4^{2-}$ ,  $\text{SeO}_3^{2-}$  and  $\text{SeO}_2^{2-}$  as radiolysis. Among the radicals, the OH radicals formed as radiolytic products of water molecules oxidize the decayed  $^{57}\text{Fe(II)}$ -species more effectively. Regarding  $\text{CoSeO}_4 \cdot \text{H}_2\text{O}$ , the relaxation time of  $^{57}\text{Fe(II)}$  to  $^{57}\text{Fe(III)}$  was estimated to be  $(51.6 \pm 3.3)$  ns, while for  $\text{CoSeO}_4$   $^{57}\text{Fe(II)}$ -2 species with a small QS value increased regarding relative intensity.

## References

- 1) W. Triftshäuser and P. P. Craig, *Phys. Rev. Lett.*, **16**, 1161 (1966); *Phys. Rev.*, **162**, 274 (1967).
- 2) W. Triftshäuser and D. Schroer, *Phys. Rev.*, **187**, 491 (1969).
- 3) G. R. Hoy, D. W. Hamill, and P. P. Wintersteiner, "Mössbauer Effect Methodology," ed by I. J. Gruverman, Plenum, New York (1970), Vol. 6, p. 109.
- 4) G. R. Hoy and P. P. Wintersteiner, *Phys. Rev. Lett.*, **28**, 877 (1972).
- 5) R. Grimm, P. Gütlich, E. Kankleit, and R. Link, *J. Chem. Phys.*, **67**, 54 (1977).
- 6) T. Kobayashi and K. Fukumura, *Nucl. Instrum. Methods*, **166**, 257 (1979).
- 7) T. Kobayashi and J. M. Friedt, *Bull. Chem. Soc. Jpn.*, **59**, 631 (1986).
- 8) T. Kobayashi, *Radiochim. Acta*, **42**, 139 (1987).
- 9) T. Kobayashi, *Bull. Chem. Soc. Jpn.*, **62**, 516 (1989).
- 10) J. Ladrière, J. C. Krack, and D. Apers, *J. Phys.*, **C2**, 434 (1979).
- 11) V. Lenher and C. H. Kao, *J. Am. Chem. Soc.*, **47**, 1521 (1925).
- 12) Y. Watanabe, K. Endo, and H. Sano, *J. Radioanal. Nucl. Chem. Lett.*, **119**, 467 (1987).
- 13) Y. Watanabe, K. Endo, and H. Sano, *Hyperfine Int.*, **42**, 1025 (1988).
- 14) Y. Watanabe, K. Endo, and H. Sano, *Bull. Chem. Soc. Jpn.*, **61**, 2785 (1988).
- 15) F. J. Lynch, R. E. Holland, and Hamermesch, *Phys. Rev.*, **120**, 513 (1960).
- 16) D. W. Hawill and G. R. Hoy, *Phys. Rev. Lett.*, **21**, 724 (1968).
- 17) Y. Watanabe, M. Nakada, K. Endo, H. Nakahara, and H. Sano, *J. Radioanal. Nucl. Chem. Lett.*, **136**, 257 (1989).
- 18) H. Sano, K. Sato, and H. Iwagami, *Bull. Chem. Soc. Jpn.*, **44**, 2570 (1971).
- 19) H. Sano and T. Ohnuma, *Chem. Phys. Lett.*, **26**, 348 (1974).
- 20) H. Sano and T. Ohnuma, *Bull. Chem. Soc. Jpn.*, **48**, 266 (1975).
- 21) H. Sano, M. Harada, and K. Endo, *Bull. Chem. Soc. Jpn.*, **51**, 2583 (1978).
- 22) K. Endo, M. Harada, Y. Sakai, and H. Sano, *J. Phys.*, **C2**, 420 (1979).
- 23) Y. Sakai, K. Endo, and H. Sano, *Bull. Chem. Soc. Jpn.*, **53**, 1317 (1980). *ibid.*, **54**, 3589 (1981).
- 24) P. W. Atkins, M. C. R. Symons, and H. W. Wardale, *J. Chem. Soc.*, **1964**, 5215.
- 25) K. Aiki, *J. Phys. Soc. Jpn.*, **29**, 379 (1970).
- 26) T. A. Carlson, *Phys. Rev.*, **131**, 676 (1963).